Journal of Alloys and Compounds 849 (2020) 156685

Contents lists available at ScienceDirect

Journal of Alloys and Compounds

journal homepage: http://www.elsevier.com/locate/jalcom

Formation and evolution of the interfacial structure in al/steel compound castings during solidification and heat treatment

Aina Opsal Bakke [a], Lars Arnberg [a], Jan-Ove Løland [b], Svein Jørgensen [b], Jan Kvinge [b], Yanjun Li [a, *]

[a] Norwegian University of Science and Technology, Department of Materials Science and Engineering, Alfred Getz' Vei 2, 7034, Trondheim, Norway
[b] Aludyne Norway, Vollmonaveien 7, 4550, Farsund, Norway

ARTICLE INFO

Article history:
Received 30 April 2020
Received in revised form
7 August 2020
Accepted 10 August 2020
Available online 13 August 2020

Keywords:
Metals and alloys
Intermetallics
Liquid-solid reactions
Microstructure

ABSTRACT

In this work, Al7SiMg/steel compound castings were produced through a low-pressure die casting process. All steel inserts were galvanized, where half of them were flux-coated to further improve the wettability and remove interfacial oxide layers during casting. The reaction layer formed in the Al7SiMg/steel interface was examined using Optical Microscopy (OM), Scanning Electron Microscopy (SEM) and Energy Dispersive X-ray Spectroscopy (EDS). In addition, Vickers Micro-hardness was measured across the interface. Results show that successful metallurgical bonding can be achieved between aluminum and galvanized steel, both with and without additional flux coating. A large fraction of intermetallic particles formed at the reaction layer, where ternary $Al_{4.5}FeSi$ particles were the dominating phase. The influence of T6 heat treatment (solution treatment at 540 °C, followed by artificial ageing) on the interfacial microstructure was also studied. After heat-treatment, the thickness of the interfacial layer increased significantly, due to the growth of β-$Al_{4.5}FeSi$ and Al−Fe binary particles into the bulk of steel. Consequently, cracks formed and propagated through the inner binary intermetallic layer. Formation mechanisms of various intermetallic phases at the interface during solidification and heat treatment have been discussed.

1. Introduction

Increasing demand in reducing climate gas emission, has led to development in the automotive industry towards more lightweight vehicles. One of the leading methods is to replace steel, which has been the main material in vehicle construction, with lighter materials. Aluminum alloys are known to have a high strength-to-weight ratio and good formability, making them excellent in automotive applications [1]. However, one material alone can often not meet the specific criteria needed in automotive components. Thus, the need for multi-material components arise.

Aluminum-steel bimetals have been considered as a potential solution for some components in the automotive industry. Various welding processes have been used in creating aluminum-steel joints, including friction stir welding [2], friction welding [3] and laser welding [4]. Recently, compound casting, a process in which a solid steel part is inserted into the mold prior to casting followed by liquid aluminum being poured and solidifies around it, has attracted more research interest. During the compound casting process, a reaction layer will form between the two materials, resulting in a metallurgical bond. Compound casting is known to have low process cost and high production efficiency. Also, there are less geometrical restrictions related to compound casting, compared to other joining processes such as welding [5]. However, due to large differences in mechanical properties and melting temperature of the two metals, and the ease of aluminum oxide forming at the joint interface, a defect-free metallic bond between aluminum and steel is difficult to achieve. In addition, the oxides on the steel insert and liquid aluminum surfaces are thermodynamically stable and have melting points greatly exceeding casting temperatures [6,7]. This will reduce the wettability of the steel surfaces to liquid aluminum, and thus inhibit formation of metallurgical bonding [8]. Furthermore, the formation of brittle intermetallic phases at the aluminum/steel interface during solidification will also reduce the bonding strength [9].

Due to the difficulty of joining aluminum and steel through a casting process, different surface treatments have been incorporated to improve bonding. Zinc has a relatively low melting point and can thus re-melt during casting, leaving an oxide-free steel surface, which increases chances of forming metallurgical bonds.

* Corresponding author.
E-mail address: yanjun.li@ntnu.no (Y. Li).

https://doi.org/10.1016/j.jallcom.2020.156685

Jiang et al. found that an application of a thin zinc layer containing 0.1 wt% Ni to steel pipes, ensured metallurgical bonding and significantly increased shear stress of the bimetallic casting. Without the zinc layer, only mechanical bonding was achieved [10]. However, the disadvantage of Zn-coating is that it will lead to a slight increase in the reaction layer thickness [11].

Nazari and Shabestari reported that it was possible to achieve metallurgical bonding using nitride coating on steel bars. The nitride layer also helped to decrease the thickness of the reaction layer at the interface, which could benefit the strength of the bimetallic component [12]. Aluminizing of the steel surface is another approach to improve bonding between aluminum and steel. Jiang et al. reported an aluminizing method where the steel surface first was modified by a 10% ammonium chloride solute, then coated with aluminum by a hot-dip aluminizing process. Continuous metallurgical bonding between the steel insert and cast aluminum was obtained. They also showed that an application of only the modifier or the aluminizing gave poor results [13].

It has been found that Al_5Fe_2 is the dominant phase forming between aluminum and steel after an aluminizing process, where the phase grows towards steel with a tongue-like morphology [2]. Intermetallic phases with high iron content, such as FeAl and Fe_3Al only form when higher process temperatures were used in the aluminizing process. These phases, however, are more desired as they show higher resistivity to fracture compared to phases with high aluminum content, Al_5Fe_2, Al_3Fe and Al_2Fe, that are deemed brittle and thus unwanted in the interface [14]. Si-containing aluminum alloys are often used in aluminizing, and it has been found that silicon favors formation of a thinner and more uniform reaction layer [15]. However, a high concentration of silicon could lead to the formation of $Al_{4.5}FeSi$ in the aluminum-steel interface, which is especially detrimental to bonding strength due to its platelet morphology causing high internal stress in the interface [16].

Heat treatment, including solution treatment and ageing, is common for cast aluminum alloys to optimize the mechanical properties. However, heat treatment of aluminum-steel compound castings is more critical due to its effect on the interface. Viala el al. observed a significant increase in the reaction layer thickness after solution treatment at 520 °C for 12 h, followed by ageing for 6 h at 170 °C. Several new Al—Fe—Si intermetallic phases formed in the heat-treated reaction layer, as well as the formation Kirkendall voids in the interface [17]. Such voids were also observed by Zhe et al. where the Kirkendall voids formed in the $\tau_6(Al_{4.5}FeSi)$/Al interface after long-term solution treatments at 535 °C [18]. Jiang et al. however, found that the shear strength of a bimetallic aluminum/steel compound casting increased with a solution temperature of 500 °C for 2 h, followed by ageing at 165 °C for 6 h. Higher solution temperatures or longer holding times caused excessive growth of the intermetallic layer and in certain cases cracks in the interface [19].

So far, most of the compound casting research has been based on small lab-scale samples. The microstructure formation and change during heat treatment has yet to be fully described in compound castings between aluminum and steel. In this work, the effect of galvanization of steel pipes on the formation of metallurgical bonds during compound casting between steel and an Al7SiMg alloy during an industrial scale low pressure die casting process, has been studied. To decrease surface oxides in the interface, a flux coating was applied in addition to the galvanized layer on some steel pipes. A detailed and systematic characterization of the interface was conducted. In addition, the effect of heat treatment on the interfacial structure evolution was examined.

2. Material and methods

Bimetallic aluminum (A356)-steel components were produced at Aludyne Norway's facilities through a vacuum/pressure riserless casting process (VRC/PRC). Chemical compositions of the A356 aluminum alloy are given in Table 1 along with the compositions of ST37 steel. ST37 steel pipes with a diameter of 10 mm, 1 mm wall thickness and length of 298 mm were inserted into a permanent mold as shown in Fig. 1.

Prior to casting, the steel pipes were galvanized through an industrial hot-dipping process. This galvanizing process follows the ISO standard NS-EN-ISO 1461, and includes degreasing in an alkaline solution followed by acid pickling before being hot-dip galvanized. Plugs were inserted into the pipes, so that only the outside surface was galvanized. The pipes were then placed in a cage and immersed into a Zn bath. After galvanizing, half of the pipes were degreased, and further flux coated using NOCOLOCK® Cs Flux. The flux was applied to investigate if removal of the oxide layer could be improved by the addition of flux coating on the galvanized steel pipes. This flux is a mixture of $K_{1-3}AlF_{3-6}$ and $CsAlF_4$ and has a melting temperature in the range of 558—566 °C [20]. It was first mixed with denatured alcohol to an alcohol/flux ratio of approximately 7.9, and then coated on the steel pipes. Before being inserted into mold, the galvanized steel inserts were also degreased.

The aluminum melt pouring temperature for each casting was measured to be 711—713 °C. Prior to casting, the steel pipes were preheated to approximately 200 °C, while the permanent mold was kept at a temperature of 300 °C. During low pressure die casting, the applied pressure was added stepwise, starting at 0.5 psig, then increasing to 1.8 and 3.0 psig before finally dropping to 0.5 psig. A water-cooling system is embedded in the mold to help control the solidification sequence and cooling rate of the castings. After casting, some of the castings were T6 heat-treated according to the industrial process applied to automotive components: solution heat treatment at 540 °C for 2 h, followed by fast quenching to 70 °C and then artificially aged at 180 °C for 2.5 h. Process parameters of the representative castings are shown in Table 2.

Samples of approximately 1 cm thickness were cut form the compound casting part for further inspection. These samples were ground and polished down to a 1 μm finish. The aluminum-steel interface was investigated using a Leica MEF4M optical microscope. A Zeiss Supra 55VP Field Emission Scanning Microscope (FESEM) with 10 mm working distance and an acceleration voltage of 15 kV was used to further characterize the interface. Energy Dispersive X-ray Spectroscopy (EDS) was used to identify the intermetallic phases formed. Vickers micro-hardness was measured across the interface of each sample using a Leica VMHT MOT micro-hardness tester with 25g load and 10 s holding time.

3. Results

3.1. Microstructure of initial galvanization layer

Fig. 2 shows a backscattered electron (BSE) micrograph of the galvanized layer prior to casting. Morphology of the layer suggests growth of intermetallic phases from the steel pipe surface. The

Table 1
Chemical composition of aluminum alloy A356 and ST37 steel.

Alloy	Composition [wt%]								
A356	Si	Mg	Ti	Fe	Sr	Ga	Zn	Others	Al
	7.0	0.41	0.11	0.082	0.013	0.0089	0.0042	0.0042	Bal.
ST37	Mn	Si	C	S	P	Fe			
	0.9	0.15—0.40	0.36	0.05	0.04	Bal.			

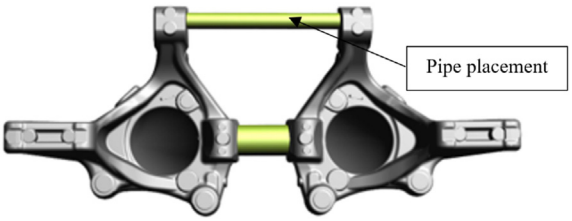

Fig. 1. The A356/steel compound casting. The steel pipe was placed in the upper yellow section as indicated by the arrow. (For interpretation of the references to colour in this figure legend, the reader is referred to the Web version of this article.)

Table 2
Process parameters for the investigated Al/steel compound castings.

Sample name	Galvanized	Flux coated	Heat treatment (T6)
A	X	–	–
B	X	–	X
C	X	X	–
D	X	X	X

galvanized layer thickness is approximately 40 μm. However, in other local regions, the thickness was up to 165 μm. This shows that the galvanizing process does not result in a uniform coating layer, which could affect bonding and formation of a reaction layer during casting.

Composition of the intermetallic layer was determined using EDS, as shown in Table 3. As can be seen, multiple phases appear to have formed in the intermetallic layer. At the steel surface, the thin intermetallic phase layer with contrast similar to the steel pipe (area 4 in Table 3) is Zn_7Fe. The remaining intermetallic layer was determined to be composed of two different phases, although only a slight contrast variation can be observed between them. $FeZn_{10}$ (area 3) appears to have formed closest to the Zn_7Fe layer, while $FeZn_{13}$ (area 2) was found growing from the $FeZn_{10}$ layer. These phases are commonly known to form during the hot dip galvanization process [21]. Outside these phases, no Fe was detected, leaving a pure zinc layer. It can also be seen from the micrograph in Fig. 2, that bonding between the galvanized layer and the steel pipe is very good. No apparent oxides can be detected by EDS in the interface.

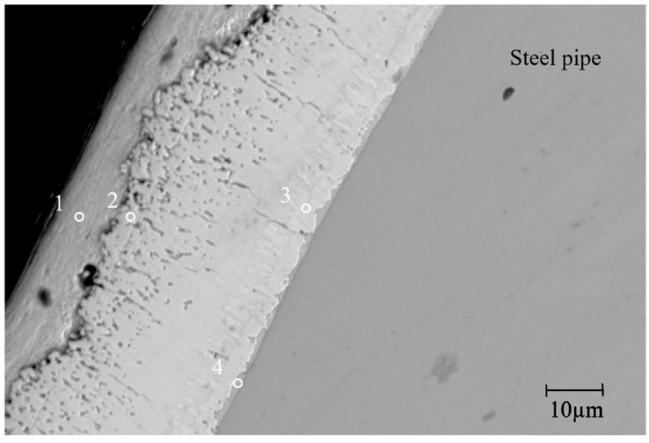

Fig. 2. BSE micrograph of the hot-dipped galvanized layer on the steel pipe prior to casting.

Table 3
Compositions and possible phases analyzed by EDS of the galvanized layer on the steel pipe prior to casting.

Area in Fig. 2	Composition [at%]		Possible phase
	Fe	Zn	
1	–	100	Zn
2	6.52	93.48	$Zn_{13}Fe$
3	9.32	90.68	$Zn_{10}Fe$
4	16.54	83.46	Zn_7Fe

3.2. As-cast interfacial microstructure

The microstructure at the aluminum-steel interface in the compound castings was investigated using light microscopy. Optical micrographs of the aluminum-steel interface in casting A and C, are shown in Fig. 3a and b, respectively. In both castings, metallurgical bonding has formed between the steel and the aluminum.

As can be seen, intermetallic particles (IMP) have formed at the steel surface. The particles have a platelet shape and can be observed growing into the cast aluminum side of the interface. In addition, some free-standing platelet particles can also be observed in the vicinity of the steel surface. These have likely formed in the aluminum melt during solidification. Length of the platelet particles vary for both castings, mainly in the range of 10–60 μm. By comparing Fig. 3a and b, it can be seen that the reaction layers with and without flux coating are quite similar. However, some minor differences can be observed. Several dark areas, believed to be pores can be observed in Fig. 3b. Although pores also are observed in casting A, they appear smaller and less frequently, which indicates better bonding when not using flux coating. A slightly higher fraction of eutectic silicon can also be observed close to the interface in casting C, followed by an area of barely any eutectic silicon. This can be due to the potassium from the flux, which is known to have a modifying effect on the eutectic silicon in Al–Si alloys [22].

Fig. 4 shows a BSE micrograph of the interfacial structure in casting A. The growth of platelet intermetallic particles from the steel pipe into the cast aluminum can be more clearly observed. An EDS analysis was conducted to determine the composition of the particles. The detected compositions in the analyzed areas are given in Table 4.

The particles in areas 2–5 show similar compositions, suggesting that the platelet particles are the ternary eutectic phase $Al_{4.5}FeSi$, also known as β-AlFeSi. The composition in area 1 does not coincide with any known phase, but due to the high contents of Fe and Si, it is likely the ternary τ_{11}-Al4Fe1.7Si phase. This layer is very thin. It should also be noted that no zinc was detected in the interfacial region, showing that the galvanized layer has re-melted and that the Fe–Zn intermetallic phases and zinc likely have dissolved and diffused into the aluminum melt during solidification. Similar results were found for casting C.

3.3. Interfacial microstructure after solution treatment

Fig. 5 shows BSE micrographs for casting B and D. As can be seen, the interfacial structure is nearly the same in the two castings. By comparing the interfacial structure in casting B (Fig. 5a) with that of casting A in Fig. 3a, it is clear to see that the interfacial structure has changed significantly as a result of the heat-treatment. In addition to the platelet β-AlFeSi particles formed during solidification, a continuous and dense intermetallic layer with a uniform thickness of approximately 80 μm has formed. Based on the contrast, it appears that the layer is Fe-rich and consists of two different phases.

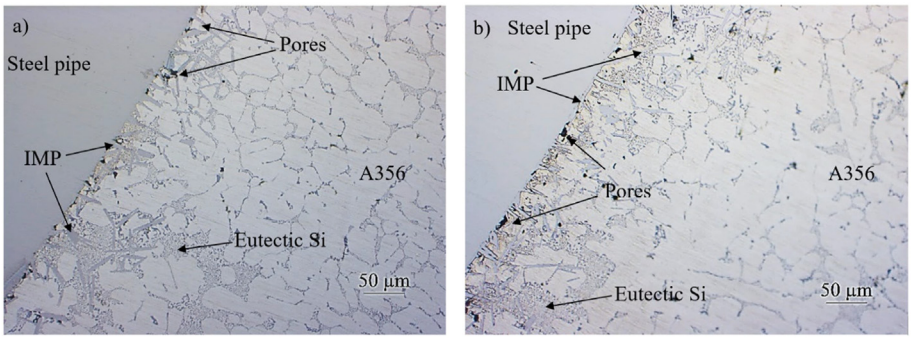

Fig. 3. Optical micrographs of the aluminum-steel interface in a) casting A, galvanized, and b) casting C, galvanized and flux coated.

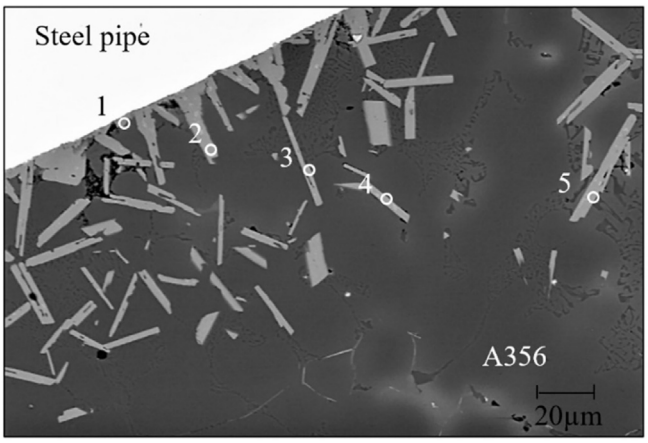

Fig. 4. Micrograph of the reaction area formed in the aluminum-steel interface in casting A.

Table 4
Compositions and possible phases analyzed by EDS of the reaction area in casting A.

Area in Fig. 4	Composition [at%]			Possible phase
	Al	Si	Fe	
1	54.75	13.14	32.11	τ_{11}-$Al_4Fe_{1.7}Si$
2	68.41	16.07	15.52	β-$Al_{4.5}FeSi$
3	68.96	16.18	14.86	β-$Al_{4.5}FeSi$
4	68.38	16.14	15.47	β-$Al_{4.5}FeSi$
5	68.33	16.15	15.52	β-$Al_{4.5}FeSi$

the aluminum casting have changed into a spherical shape. Compared to the as-cast state, the area fraction of eutectic Si particles at the vicinity of the reaction layer is much smaller.

Table 5 shows the compositions determined from the EDS analysis of the labelled areas in Fig. 5. The compositions suggest that in both castings a binary Al–Fe phase has formed closest to the steel surface. Although the composition of the inner layer in casting B (area B-4) shows a somewhat lower concentration of Fe than in casting D (areas D-3 and D-4), it is possible that the same phase, θ-Al_3Fe or η-Al_5Fe_2, has formed in both castings. In previous aluminizing experiments, an Al/Fe ratio below 2.6 was reported as η-Al_5Fe_2 [15,23], but as θ-Al_3Fe and η-Al_5Fe_2 have very similar compositions, it is difficult to distinguish them barely through EDS. However, both phases are deemed brittle, which could explain the crack propagating through this binary Al–Fe phase layer. The chemical composition of the intermetallic layer with a slightly lower contrast (areas B-2 and D-2) is very close to

Table 5
Compositions and possible phases analyzed by EDS of the reaction areas in the heat-treated castings B and D.

Casting-Area in Fig. 5	Composition [at%]				Possible phase
	Al	Si	Fe	Zn	
B-1	67.92	17.43	12.43	2.25	β-$Al_{4.5}FeSi$
B-2	68.59	18.40	13.01	-	β-$Al_{4.5}FeSi$
B-3	71.07	10.20	18.73	-	α-$Al_{7.4}Fe_2Si$
B-4	75.91	1.96	22.13	-	θ-Al_3Fe
D-1	67.60	17.44	14.96	-	β-$Al_{4.5}FeSi$
D-2	66.90	17.76	15.33	–	β-$Al_{4.5}FeSi$
D-3	70.23	3.30	26.46	–	η-Al_5Fe_2
D-4	70.88	1.66	27.46	–	η-Al_5Fe_2

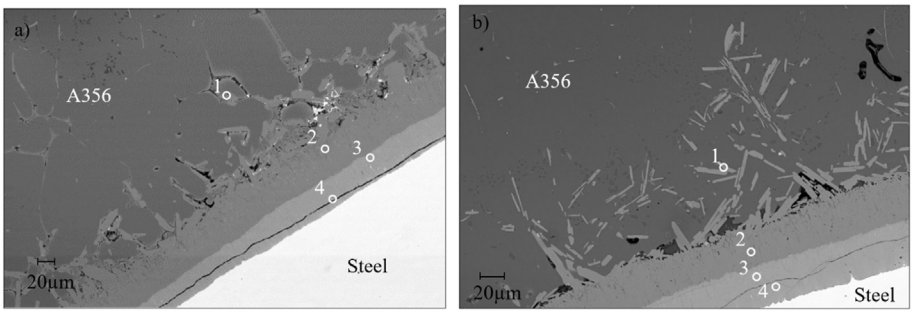

Fig. 5. Micrographs of the reaction layer formed in the aluminum-steel interface after heat-treatment for a) casting B, galvanized, and b) casting D, galvanized and flux-coated.

Additionally, cracks can be seen in the intermetallic layer with relatively higher contrast closest to the steel surface, which suggests that cracking has occurred during heat-treatment. Another change is that the fibrous shaped eutectic Si particles in the bulk of that of the ternary β-$Al_{4.5}FeSi$ phase, showing that a significant growth of the β-particles has occurred during heat treatment.

Higher magnification micrographs were captured to further study the structure of the intermetallic layer adjacent to the steel

pipe in the heat-treated castings. Fig. 6 shows the interface between the inner and outer intermetallic layer in casting B. A thin intermetallic layer can be observed between the ternary β-$Al_{4.5}FeSi$ layer and the binary Al—Fe layer. The thin layer has a higher contrast than the former phase and a slightly lower contrast than the latter phase. Also, the inner Al—Fe intermetallic layer is not homogeneous, where the varying contrast suggests growth of multiple intermetallic phases. These phases were investigated through EDS. Results are shown in Table 6.

The EDS analysis suggests that the reaction layer closest to the β-$Al_{4.5}FeSi$ layer (area 1), is the ternary τ_{11}-$Al_4Fe_{1.7}Si$ phase based on its high Fe concentration. Area 2 detects a low concentration of Si, suggesting instead formation of a binary Al—Fe phase. The composition in this area coincides with the formation of θ-Al_3Fe and it can be seen that the contrast in this phase differs from the ternary τ_{11}-$Al_4Fe_{1.7}Si$ phase and the intermetallic layer at the steel surface. This layer is determined to be binary η-Al_5Fe_2 phase (area 3), which can also be recognized in the micrograph through its tongue-like morphology growing towards the steel pipe. Also, the crack can be seen propagating through this phase. It should also be noted that although several binary Al—Fe and ternary Al—Fe—Si phases have formed, there is still some detection of Zn, showing that Zn has not diffused or dissolved completely into the cast aluminum.

3.4. Vickers micro-hardness

Micro-hardness was measured across the reaction layer for each casting. Fig. 7 shows the hardness in the as cast and heat-treated galvanized samples and their respective indentations. Similar measurements were also made for the flux-coated and galvanized samples. The indentations across casting A and casting B can be seen in Fig. 7a and b, respectively. For each casting, zero represents the interface between the steel surface and the reaction layer. It can be seen in Fig. 7c that the hardness in the reaction layer has significantly increased in the heat-treated compound casting. The inner reaction layer formed during heat treatment shows the highest hardness of approximately 1200HV, which is almost six times higher than the cast aluminum. It can also be seen that the hardness in the cast aluminum increased from the as-cast to heat-treated state, from 135 to 175 HV in average.

4. Discussion

4.1. Effect of surface treatment

The microstructure study of the galvanized layer shows that upon hot-dip galvanizing, binary Fe—Zn phases, such as $FeZn_7$, $FeZn_{10}$ and $FeZn_{13}$ form. $FeZn_{10}$ and $FeZn_{13}$ are usually the first phases to form during galvanization [21], whereas $FeZn_7$, known as δ_{1k}, is a phase with similar crystal structure as $FeZn_{10}$, δ_{1p}, and they form through the same peritectic reaction [24]. In certain areas the thickness of the galvanized layer exceeded 100 μm. Nonetheless, the EDS analyses barely show detection of zinc in the interface after casting. The pouring temperature of 700 °C during casting is above the peritectic temperatures of the detected phases in the Zn—Fe phase diagram, 672 °C and 530 °C for $FeZn_7$/$FeZn_{10}$ and $FeZn_{13}$ respectively [25]. This would allow the phases to re-melt upon casting. According to the binary Al—Zn phase diagram, Zn has a maximum solubility of 67 at% in the Al phase [26]. As no Zn-rich phase could be detected in the compound casting interface, most of the zinc and Fe—Zn phases may have immediately dissolved into the aluminum melt by diffusion and convection. This could explain why only low concentrations of zinc were detected in the interface.

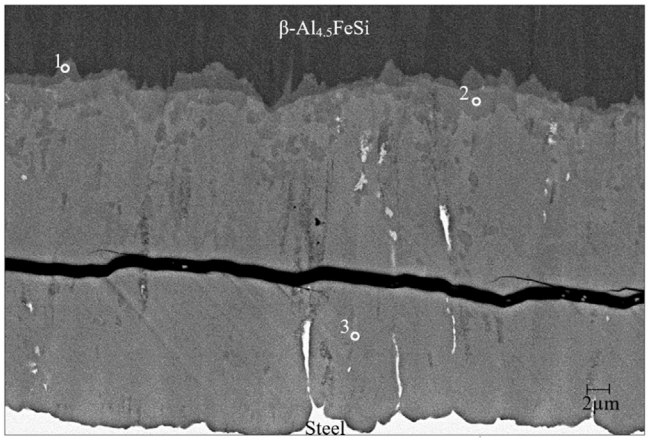

Fig. 6. Micrograph of the intermetallic layer growth in casting B.

Table 6
Compositions and possible phases analyzed by EDS of the phases observed in the intermetallic layer in casting B.

Area in Fig. 6	Composition [at%]				Possible phase
	Al	Si	Fe	Zn	
1	52.88	17.56	29.56	–	τ_{11}-$Al_4Fe_{1.7}Si$
2	72.23	4.44	21.71	1.61	θ-Al_3Fe
3	68.70	2.36	27.07	1.88	η-Al_5Fe_2

NOCOLOCK® Cs flux is commonly used for brazing aluminum alloys. When the flux reaches its melting temperature range of 558°C—566 °C, it will start reacting with the surface oxides, thus improving wettability and enhancing the formation of a metallurgical bond. However, in a brazing process, the process temperature will be held at a longer time compared to a casting process where cooling occurs immediately. This could explain why there is little difference in the interface with and without flux. Although the interfaces show only slight variations, intermetallic phases have formed in both cases, suggesting that additional flux coating was not necessary to achieve a metallurgical bond. Zinc has a melting point of 420 °C [6]. Thus, the galvanized layer will start to re-melt before the melting temperature of the flux is reached. This would imply that the flux has yet to be activated when the galvanized layer starts to melt, and it will therefore not be able to react with the surface oxides. In the re-melting process, parts of the flux might become entrapped, which could then cause some porosity at the interface. This would explain why the bonding appears to be slightly worse for the flux-coated sample. The galvanized layer will also allow liquid aluminum to react with a fresh steel surface, as the galvanized layer will prevent the steel from oxidizing. Thus, upon casting, when the galvanized layer melts, it will provide the necessary wetting of the steel surface.

4.2. Formation of the intermetallic layer during casting

During compound casting, the galvanized (Fe—Zn) layer will be melted by the liquid aluminum, resulting in a locally high concentration of Fe in the aluminum melt close to the steel surface. At the same time, direct exposure of the steel surface to the liquid aluminum can lead to formation of iron-rich intermetallic particles that grow into the liquid aluminum upon solidification. In principle, various Al—Fe intermetallic phases could form. However, as there is a high Si content (7 wt%) in the A356 casting alloy, formation of the ternary eutectic β-$Al_{4.5}FeSi$ phase is more favorable energetically. No binary Al—Fe intermetallic phases have formed in the present compound castings, which differs from the interfacial structure detected between the aluminized layer and steel formed by hot dipping in a liquid

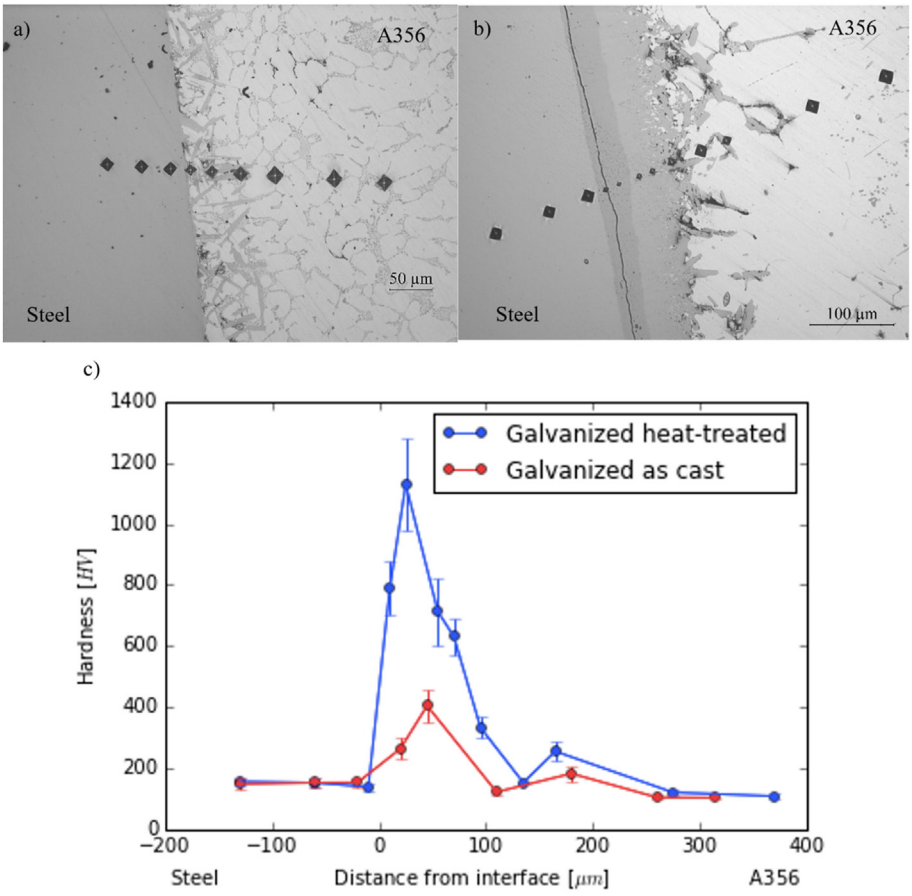

Fig. 7. Vickers micro-hardness measured across the aluminum-steel interface in the galvanized castings. a) Indentations across casting A, galvanized, b) Indentations across casting B, galvanized and heat-treated, and c) Hardness measured for each indentation.

Al—Si alloy [15]. This can be ascribed to the interfacial reaction layer remaining at an elevated temperature for a shorter time in the casting process compared to hot-dip aluminizing. Thus, the time is insufficient for η-Al_5Fe_2 or θ-Al_3Fe to form in the interface. Although the platelet-shaped β-$Al_{4.5}FeSi$ particles appear to grow from the steel surface towards the cast aluminum, some free-standing particles were also observed detached from the steel surface. Those free-standing β-$Al_{4.5}FeSi$ particles may have detached from the particles growing from the steel surface or be connected to the interfacial particles beneath the sample surface.

For both the uncoated and flux-coated castings, the main phase formed in the interface is the ternary eutectic β-$Al_{4.5}FeSi$. This phase is characterized by its platelet morphology, which in micrographs appears as needle- or plate-shaped. Due to this morphology, the β-phase is unwanted in the interface as the sharp edges can induce stress concentration and thus decrease bonding strength [16]. In addition, the length of the β-particles is also detrimental to the ultimate tensile strength, as it allows for easy crack propagation along the particle. Ma et al. reported a significant decrease in ultimate tensile strength of cast Al—Si—Cu and Al—Si—Mg alloys as the particle lengths increased to 70 µm [27]. Although the particles were found to have varying length and thickness in both compound castings with and without flux coating, the particle density is still on a level that is likely to decrease bonding strength.

4.3. Effect of heat treatment

After heat-treatment, there is a clear change in the interfacial microstructure compared to the as-cast samples. A thick layer of binary Al—Fe intermetallic particles and a denser layer of β-$Al_{4.5}FeSi$ particles have formed between the aluminum casting and the steel surface. A closer look at the interface between the two dominating intermetallic phases in the reaction layer reveals the irregular growth front of additional phases. Formation of all the intermetallic phases is attributed to the long holding time at an elevated temperature during solution treatment, which allows new intermetallic layers to form through solid-state diffusion. The β-$Al_{4.5}FeSi$ layer can have formed through further growth of the pre-existing β-particles in both the lateral direction and perpendicular direction towards the steel. In this process, the diffusion of Al and Si atoms from the aluminum grains is important, as a larger concentration of Si atoms in the aluminum grain will be consumed. This is also the reason that a large fraction of eutectic silicon particles in the vicinity of the interface have dissolved during heat treatment, as seen in Fig. 5. Due to the limited concentration of silicon in the aluminum grains at the interface, the growth of β-$Al_{4.5}FeSi$ will stop at a certain length. Instead, τ_{11}-$Al_4Fe_{1.7}Si$ particles, which have less Si content, will form and grow. With further reduction of the available Si content, binary Al—Fe phases, such as θ-Al_3Fe and η-Al_5Fe_2, form and grow into the bulk steel, which will be controlled by the diffusion of Al atoms through the grain boundaries of the β-$Al_{4.5}FeSi$ and τ_{11}-$Al_4Fe_{1.7}Si$ particles. This is similar to the formation of the aluminized layer during hot-dipping of steel in aluminum alloys. In the hot-dipping process, it was found that a high silicon content in the aluminum alloy can significantly reduce the thickness of the Al—Fe intermetallic layer [15]. Here, a significant growth of the intermetallic layer has occurred during heat treatment, despite the cast A356 alloy having 7 wt% Si. This is due to the long

holding time at an elevated temperature during solution treatment, which allows for long-range diffusion of Al and Si atoms. θ-Al_3Fe has lower Gibbs free energy and is therefore expected to form prior to η-Al_5Fe_2 [28]. However, experimentally it is often observed that η-Al_5Fe_2 is the dominant phase forming between Al and Fe both in solid/solid and solid/liquid diffusion bonding and through friction stir welding [2,9], having a distinctive tongue-like morphology extending towards the iron/steel side. It has also been suggested that due to η-Al_5Fe_2 having an orthorhombic crystal structure with several aluminum vacancies in the c-axis, diffusion is more rapid in this phase than for θ-Al_3Fe, which is monoclinic [28]. This favors the significant growth of the η-Al_5Fe_2 phase. In the interface between the two dominating intermetallic layers after heat treatment, it was determined that both η-Al_5Fe_2 and θ-Al_3Fe formed (Table 6). Si can in general slow down the growth of the reaction layer, but it has also been found to alter the diffusion conditions of the η-Al_5Fe_2 phase, which then could allow formation of θ-Al_3Fe instead [29]. Nonetheless, both phases are deemed brittle [14].

It should be mentioned that the growth of the interfacial intermetallic layer formed in the compound castings after heat treatment, is similar to that observed during solid/solid diffusion bonding between steel and aluminum, where the thickness of the intermetallic layer increases with temperature and holding time [9,30]. Jiang et al. also observed the increasing thickness with higher solution treatment temperatures in a compound casting process between an Al–Si alloy and steel, but the irregularity of the intermetallic phase closest to the cast aluminum alloy remained through heat treatment [31]. Although a uniform intermetallic layer can be beneficial compared to the stress-inducing particles observed in an irregular layer and the as-cast samples, a thicker layer would in general be detrimental to the overall bonding strength due to formation of brittle intermetallic phases. Additionally, the brittle intermetallic phases are more prone to cracking compared to the bulk aluminum. Jiang et al. also observed formation of a crack through the reaction layer with solution treatment times of 6 and 10 h [31]. The crack formation was attributed to the build-up of thermal stress at the interface during quenching due to the different thermal expansion coefficients of aluminum, steel and interfacial intermetallic phases, which results in crack formation and propagation through the brittle intermetallic phases [32,33]. A higher solution temperature or longer solution treatment will cause a significant thickening of the intermetallic layer at the interface. A thicker layer of the brittle intermetallic phase will cause higher stress and thus easier formation and propagation of fracture. Although the solution treatment time in the present research was only 2 h, the temperature of 540 °C is relatively high. Therefore, a traditional T6 treatment is not recommended for steel-aluminum compound castings. A T5 treatment or a much lower solution treatment temperature and time, as suggested in Ref. [19,31] will reduce the trend of crack formation by avoiding the significant intermetallic layer growth.

5. Conclusions

Successful metallurgical bonding has been achieved in compound castings between aluminum alloy A356 and galvanized steel by an industrial scale low pressure die casting method. Additional flux coating of the galvanized steel inserts showed no significant improvement on the final interfacial microstructure, likely due to the higher melting temperature needed for melting of the flux coating than the galvanized layer.

During compound casting, both the Zn-layer and the binary Fe–Zn phases in the galvanized layer completely dissolved into the cast aluminum alloy.

At the interface between the A356 aluminum alloy and the steel insert, a thin reaction layer consisting of ternary τ_{11}-$Al_4Fe_{1.7}Si$ and binary θ-Al_3Fe particles formed after compound casting. These intermetallic particles are believed to grow from the steel surface into the aluminum melt during solidification.

A T6 heat-treatment can significantly improve the Vickers hardness of the cast aluminum. However, it induces a considerable increase of the intermetallic layer thickness at the interface. The thick interfacial reaction layer has formed though solid-state diffusion during solution treatment and consists of a binary Al–Fe intermetallic layer, a ternary β-$Al_{4.5}FeSi$ layer and a thin layer consisting of τ_{11}-$Al_4Fe_{1.7}Si$ and θ-Al_3Fe in between. Cracks were found to form and easily propagate in the brittle Al–Fe intermetallic layer, which suggests that a high solution treatment temperature is not suitable for aluminum-steel compound castings.

CRediT authorship contribution statement

Aina Opsal Bakke: Validation, Investigation, Writing - original draft, Visualization. **Lars Arnberg:** Supervision, Writing - review & editing, Visualization. **Jan-Ove Løland:** Funding acquisition, Project administration, Methodology, Resources. **Svein Jørgensen:** Methodology, Resources. **Jan Kvinge:** Methodology, Resources. **Yanjun Li:** Supervision, Writing - review & editing, Visualization.

Declaration of competing interest

The authors declare that they have no known competing financial interests or personal relationships that could have appeared to influence the work reported in this paper.

Acknowledgements

The Research Council of Norway is the main funding source for this work. The support is given to the IPN project AluLean with project number 90141902. Aludyne Norway has contributed with materials and casting facilities.

Appendix A. Supplementary data

Supplementary data to this article can be found online at https://doi.org/10.1016/j.jallcom.2020.156685.

References

[1] W. Miller, L. Zhuang, J. Bottema, A. Wittebrood, P. De Smet, A. Haszler, A. Vieregge, Recent development in aluminum alloys for the automotive industry, Mater. Sci. Eng. A 280 (2000) 37–49, https://doi.org/10.1016/S0921-5093(99)00653-X.
[2] H. Springer, A. Kostka, J.F. dos Santos, D. Raabe, Influence of intermetallic phases and Kirkendall-porosity on the mechanical properties of joints between steel and aluminium alloys, Mater. Sci. Eng. A 528 (2011) 4630–4642, https://doi.org/10.1016/j.msea.2011.02.057.
[3] S. Herbst, H. Aengeneyndt, H.J. Maier, F. Nürnberger, Microstructure and mechanical properties of friction welded steel-aluminum hybrid components after T6 heat treatment, Mater. Sci. Eng. A 696 (2017) 33–41, https://doi.org/10.1016/j.msea.2017.04.052.
[4] L. Jia, J. Shichun, S. Yan, N. Cong, C. Junke, H. Genzhe, Effects of zinc on the laser welding of an aluminum alloy and galvanized steel, J. Mater. Process. Technol. 224 (2015) 49–59, https://doi.org/10.1016/j.jmatprotec.2015.04.017.
[5] R.K. Tayal, V. Singh, S. Kumar, R. Garg, Compound casting - a literature review, Proceeding. National Conferen. Trend. Adv. Mechan. Eng. (2012) 501–510.
[6] G. Aylward, T. Findlay, SI Chemical Data, fifth ed., John Wiley & Sons Australia, Milton, 2002.
[7] K.J.M. Papis, J.F. Loeffler, P.J. Uggowitzer, Light metal compound casting, Sci. China, Ser. A 52 (2009) 46–51.
[8] K.J.M. Papis, B. Hallstedt, J.F. Löffler, P.J. Uggowitzer, Interface formation in aluminum-aluminum compound casting, Acta Mater. 56 (2008) 3036–3043, https://doi.org/10.1016/j.actamat.2008.02.042.
[9] H. Springer, A. Kostka, E.J. Payton, D. Raabe, A. Kaysser-Pyzalla, G. Eggeler, On the formation and growth of intermetallic phases during interdiffusion between low-carbon steel and aluminum alloys, Acta Mater. 59 (2011)

1586–1600, https://doi.org/10.1016/j.actamat.2010.11.023.
[10] W. Jiang, Z. Fan, G. Li, C. Li, Effects of zinc coating on interfacial microstructures and mechanical properties of aluminum/steel bimetallic composites, J. Alloys Compd. 678 (2016) 249–257, https://doi.org/10.1016/j.jallcom.2016.03.276.
[11] H. Springer, A. Szczepaniak, D. Raabe, On the role of zinc on the formation and growth of intermetallic phases during interdiffusion between steel and aluminum alloys, Acta Mater. 96 (2015) 203–211, https://doi.org/10.1016/j.actamat.2015.06.028.
[12] K.A. Nazari, S.G. Shabestari, Effect of micro alloying elements on the interfacial reactions between molten aluminum alloy and tool steel, J. Alloys Compd. 478 (2009) 523–530, https://doi.org/10.1016/j.jallcom.2008.11.127.
[13] W. Jiang, Z. Fan, C. Li, Improved steel/aluminum bonding in bimetallic castings by a compound casting process, J. Mater. Process. Technol. 226 (2015) 25–31, https://doi.org/10.1016/j.jmatprotec.2015.06.032.
[14] S. Kobayashi, T. Yakou, Control of intermetallic compound layers at interface between steel and aluminum by diffusion-treatment, Mater. Sci. Eng. A 338 (2002) 44–53, https://doi.org/10.1016/S0921-5093(02)00053-9.
[15] W.-J. Cheng, C.-J. Wang, Effect of silicon on the formation of intermetallic phases in aluminide coating on mild steel, Intermetallics 19 (2011) 1455–1460, https://doi.org/10.1016/j.intermet.2011.05.013.
[16] S. Seifeddine, S. Johansson, I.L. Svensson, The influence of cooling rate and manganese content on the β-Al5FeSi phase formation and mechanical properties of Al-Si-based alloys, Mater. Sci. Eng. A 490 (2008) 385–390, https://doi.org/10.1016/j.msea.2008.01.056.
[17] J.C. Viala, M. Peronnet, F. Barbeau, F. Bosselet, J. Bouix, Interface chemistry in aluminium alloy castings reinforced with iron base inserts, Compos. Part A Appl. Sci. Manuf. 33 (2002) 1417–1420, https://doi.org/10.1016/S1359-835X(02)00158-6.
[18] M. Zhe, O. Dezellus, B. Gardiola, M. Braccini, J.C. Viala, Chemical changes at the interface between low carbon steel and an Al-Si alloy during solution heat treatment, J. Phase Equilibria Diffus. (2011) 486–497, https://doi.org/10.1007/s11669-011-9949-z.
[19] W. Jiang, G. Li, Y. Wu, X. Liu, Z. Fan, Effect of heat treatment on bonding strength of aluminum/steel bimetal produced by compound casting, J. Mater. Process. Technol. 258 (2018) 239–250, https://doi.org/10.1016/j.jmatprotec.2018.04.006.
[20] S.A. Solvay, Safety data sheet - NOCOLOK®Cs FLUX (TM) BW. https://www.solvay.us/en/binaries/P36966-USA_CN_EN3-238040.pdf, 2017. (Accessed 5 February 2018).
[21] P. Pokorny, P. Kolisko, L. Balik, P. Novak, Reaction kinetics of the formation of intermetallic Fe-Zn during hot-dip galvanizing of steel, Metalurgija 55 (2016) 111–114.
[22] M.D. Hanna, S.-Z. Lu, A. Hellawell, Modification in the aluminum silicon system, Metall. Trans. A 15 (1984) 459–469, https://doi.org/10.1007/BF02644969.
[23] W.-J. Cheng, C.-J. Wang, Observation of high-temperature phase transformation in the Si-modified aluminide coating on mild steel using EBSD, Mater. Char. 61 (2010) 467–473, https://doi.org/10.1016/j.matchar.2010.02.001.
[24] P. Pokorny, J. Kolisko, L. Balik, P. Novak, Description of structure of Fe-Zn intermetalic compounds present in hot-dip galvanized coatings on steel, Metalurgija 54 (2015) 707–710.
[25] H. Baker, H. Okamoto, Binary alloy phase diagrams, in: ASM Handbook, Volume 03 - Alloy Phase Diagrams, ASM International, 1992, p. 206.
[26] J.L. Murray, The Al-Zn (Aluminum-Zinc) system, Bull. Alloy Phase Diag. 4 (1983) 55–73, https://doi.org/10.1007/BF02880321.
[27] Z. Ma, A.M. Samuel, F.H. Samuel, H.W. Doty, S. Valtierra, A study of tensile properties in Al-Si-Cu and Al-Si-Mg alloys: effect of β-iron intermetallics and porosity, Mater. Sci. Eng. A (2008) 36–51, https://doi.org/10.1016/j.msea.2008.01.028.
[28] H.R. Shahverdi, M.R. Ghomashchi, S. Shabestari, J. Hejazi, Microstructural analysis of interfacial reaction between molten aluminum and solid iron, J. Mater. Process. Technol. 124 (2002) 345–352, https://doi.org/10.1016/S0924-0136(02)00225-X.
[29] G. Eggeler, W. Auer, H. Kaesche, On the influence of silicon on the growth of the alloy layer during hot dip aluminizing, J. Mater. Sci. 21 (1986) 3348–3350, https://doi.org/10.1007/BF00553379.
[30] K. Bhanumurthy, W. Krauss, J. Konys, Solid-state diffusion reaction and formation of intermetallic phases in the Fe-Al system, Fusion Sci. Technol. 65 (2014) 262–272, https://doi.org/10.13182/FST13-651.
[31] W. Jiang, G. Li, Z. Jiang, Y. Wu, Z. Fan, Effect of heat treatment on microstructures and mechanical properties of Al/Fe bimetal, Mater. Sci. Technol. 34 (2018) 1519–1528, https://doi.org/10.1080/02670836.2018.1465620.
[32] Q. Wang, X.-s. Leng, T.-h. Yang, J.-c. Yan, Effects of Fe—Al intermetallic compounds on interfacial bonding of clad materials, Trans. Nonferrous Metals Soc. China 24 (2014) 279–284, https://doi.org/10.1016/S1003-6326(14)63058-2.
[33] J.Y. Jin, S.I. Hong, Effect of heat treatment on tensile deformation characteristics and properties of Al3003/STS439 clad composite, Mater. Sci. Eng., A 596 (2014) 1–8, https://doi.org/10.1016/j.msea.2013.12.019.